ISCI, Volume *21*

Supplemental Information

2-Methylthio Conversion of N6-Isopentenyladenosine in Mitochondrial tRNAs by CDK5RAP1 Promotes the Maintenance of Glioma-Initiating Cells

Takahiro Yamamoto, Atsushi Fujimura, Fan-Yan Wei, Naoki Shinojima, Jun-ichiro Kuroda, Akitake Mukasa, and Kazuhito Tomizawa

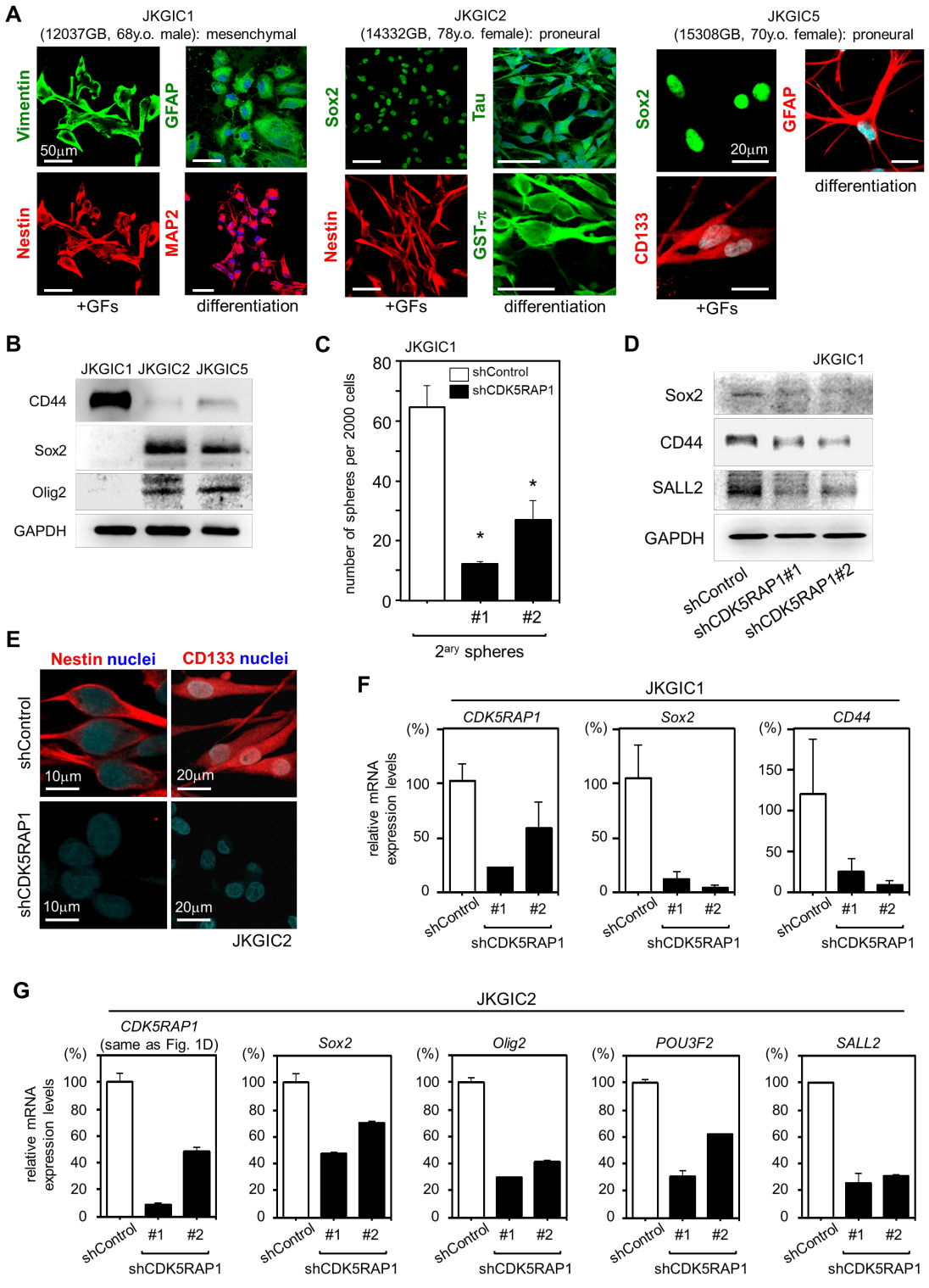
A
JKGIC1
(12037GB, 68y.o. male): mesenchymal
JKGIC2
(14332GB, 78y.o. female): proneural
JKGIC5
(15308GB, 70y.o. female): proneural
Vimentin
GFAP
Sox2
Tau
Sox2
GFAP
50μm
20μm
Nestin
MAP2
Nestin
GST-π
CD133
+GFs
differentiation
+GFs
differentiation
+GFs
differentiation
B
JKGIC1 JKGIC2 JKGIC5
CD44
Sox2
Olig2
GAPDH
C
JKGIC1
shControl
shCDK5RAP1
number of spheres per 2000 cells
80
60
40
20
0
*
*
#1
#2
2ary spheres
D
JKGIC1
Sox2
CD44
SALL2
GAPDH
shControl
shCDK5RAP1#1
shCDK5RAP1#2
E
Nestin nuclei
CD133 nuclei
shControl
shCDK5RAP1
10μm
20μm
10μm
20μm
JKGIC2
F
JKGIC1
CDK5RAP1
Sox2
CD44
(%)
relative mRNA expression levels
100
50
0
150
shControl
#1
#2
shCDK5RAP1
G
JKGIC2
CDK5RAP1
(same as Fig. 1D)
Sox2
Olig2
POU3F2
SALL2
(%)
relative mRNA expression levels
100
80
60
40
20
0
shControl
#1
#2
shCDK5RAP1

Figure S1. CDK5RAP1 is required to sustain the GIC-related traits and the transcriptional regulation of the GIC markers. (related to Figure 1).

(A-B) Molecular characteristics of JKGIC1, JKGIC2 and JKGIC5 cells. (A) Immunocytochemical analysis for GIC (Vimentin, Sox2, Nestin and CD133), neural (MAP2 and Tau), astrocytic (GFAP) and oligodendrocytic (GST-π) markers. (B) Western blotting for CD44, Sox2, and Olig2 in each cell. CD44 is abundantly expressed in JKGIC1 cells, whereas Sox2 and Olig2 are predominately expressed in JKGIC2 and JKGIC5 cells. All cell lines can differentiate into several lineages, such as neuronal, astrocytic and oligodendrocytic lineages.

(C) Quantification of secondary sphere formation by shControl-, shCDK5RAP1#1-, and shCDK5RAP1#2-transfected JKGIC1 cells. CDK5RAP1 is required to sustain the anchorage-independent growth capacity of JKGIC1 cells. The data are presented as the number of spheres formed from 2,000 seeded cells. Each bar represents the SD value from four independent replicates. *: $P<0.05$ *vs.* shControl.

(D) CDK5RAP1 knockdown decreases the expression levels of transcriptional regulators of GIC markers in JKGIC1.

(E) Representative immunostaining images for each stem cell marker in shControl- and shCDK5RAP1-transfected JKGIC2 cells. Cells were dispersed on Matrigel® Matrix (Corning, Bedford, MA), and then immunocytochemical analysis was performed. CDK5RAP1 deficiency results in reduced staining for Nestin and CD133.

(F-G) CDK5RAP1 deficit reduces the expression levels of GIC-related transcriptional factors in JKGIC1 and JKGCI2. Each bar represents the SD value from three independent replicates.

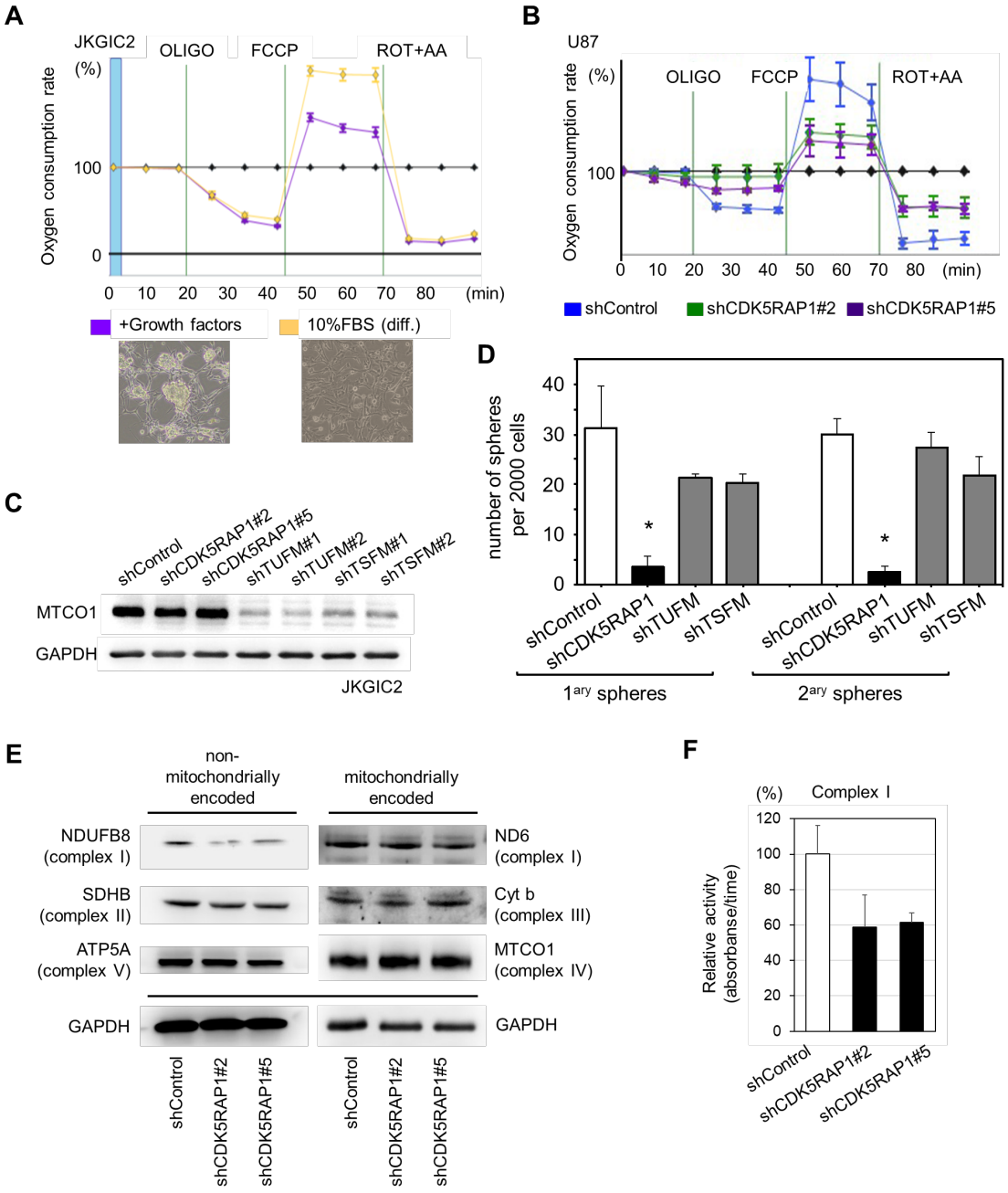
A
JKGIC2
OLIGO
FCCP
ROT+AA
(%)
Oxygen consumption rate
100
0
0 10 20 30 40 50 60 70 80 (min)
+Growth factors
10%FBS (diff.)
B
U87
(%)
OLIGO
FCCP
ROT+AA
Oxygen consumption rate
100
0 10 20 30 40 50 60 70 80 (min)
shControl
shCDK5RAP1#2
shCDK5RAP1#5
C
shControl
shCDK5RAP1#2
shCDK5RAP1#5
shTUFM#1
shTUFM#2
shTSFM#1
shTSFM#2
MTCO1
GAPDH
JKGIC2
D
number of spheres per 2000 cells
40
30
20
10
0
*
*
shControl
shCDK5RAP1
shTUFM
shTSFM
shControl
shCDK5RAP1
shTUFM
shTSFM
1ary spheres
2ary spheres
E
non-mitochondrially encoded
mitochondrially encoded
NDUFB8 (complex I)
SDHB (complex II)
ATP5A (complex V)
GAPDH
ND6 (complex I)
Cyt b (complex III)
MTCO1 (complex IV)
GAPDH
shControl
shCDK5RAP1#2
shCDK5RAP1#5
shControl
shCDK5RAP1#2
shCDK5RAP1#5
F
(%) Complex I
Relative activity (absorbanse/time)
120
100
80
60
40
20
0
shControl
shCDK5RAP1#2
shCDK5RAP1#5

Figure S2. CDK5RAP1 controls GIC-related traits in a mitochondrial translation-independent manner (related to Figure 2).

(A) *Upper panel*: Representative oxygen consumption rates in JKGIC2 cells cultured in GIC medium containing bFGF and EGF (+GF) or differentiation medium containing 10% FBS. Upon exposure to a differentiation cue, respiratory coupling was significantly induced after FCCP treatment in differentiated JKGIC2 cells. n = 5 per condition. *Lower panel*: Representative images of undifferentiated (purple) and differentiated (orange) JKGIC2 cells.

(B) Representative oxygen consumption rates in U87MG cells transfected with shControl, shCDK5RAP1#2, or shCDK5RAP1#5. In contrast to that in JKGIC2 cells, CDK5RAP1 deficiency induced a marked change in the OCR in the non-GIC line. n=5 per condition.

(C) Immunoblots for MTCO1 in JKGIC2 cells transfected with each shRNA. GAPDH served as a loading control.

(D) Knockdown of CDK5RAP1 represses the anchorage-independent growth ability of JKGIC2 cells. In contrast, knockdown of either TUFM or TSFM has no effect on the self-renewal capacity of JKGIC2 cells. Each bar represents the SD value from four independent replicates. *: $P<0.05$ *vs.* shControl.

(E) CDK5RAP1 deficit slightly attenuated the protein level of NDUFB8, but had no effect on other component proteins in JKGIC2. Note that the levels of proteins encoded by mitochondrial genome such as ND6, cytochrome b, and MTCO1 were not reduced upon loss of CDK5RAP1.

(F) Complex I activity was reduced upon CDK5RAP1 knockdown.

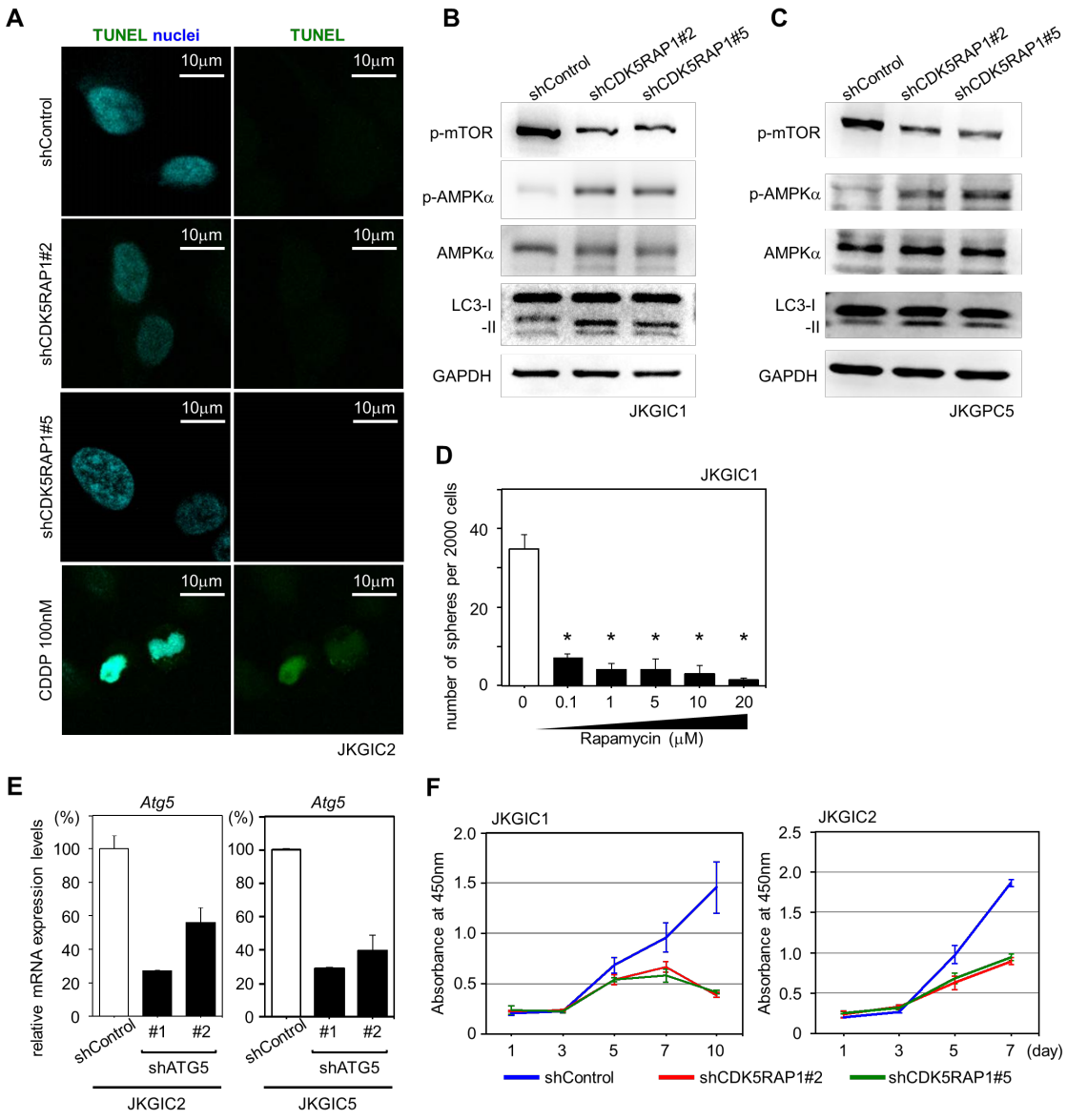

Figure S3. CDK5RAP1 knockdown inhibits the growth of GICs but does not induce apoptosis in GICs (related to Figure 3).

(A) Representative images of TUNEL assays in JKGIC2 cells transfected with shControl or shCDK5RAP1#2. Note that CDK5RAP1 knockdown does not activate apoptosis. CDDP-treated JKGIC2 cells served as a positive control for the TUNEL assay.

(B-C) Immunoblotting analyses of mTOR, AMPK, and LC3 show that CDK5RAP1 knockdown activates the autophagic program in JKGIC1 and JKGCI5 cells.

(D) Dose-dependent effect of rapamycin on the number of spheres formed from 2,000 JKGIC1 cells. Each bar represents the SD value from four independent replicates. *: $P<0.05$.

(E) The efficiency of shATG5 was examined by real-time PCR in JKGIC2 and JKGIC5 cells. n = 5 per condition.

(F) CDK5RAP1 knockdown inhibits the growth of both JKGIC1 and JKGIC2 cells. Cell growth was measured by the WST-8 assay.

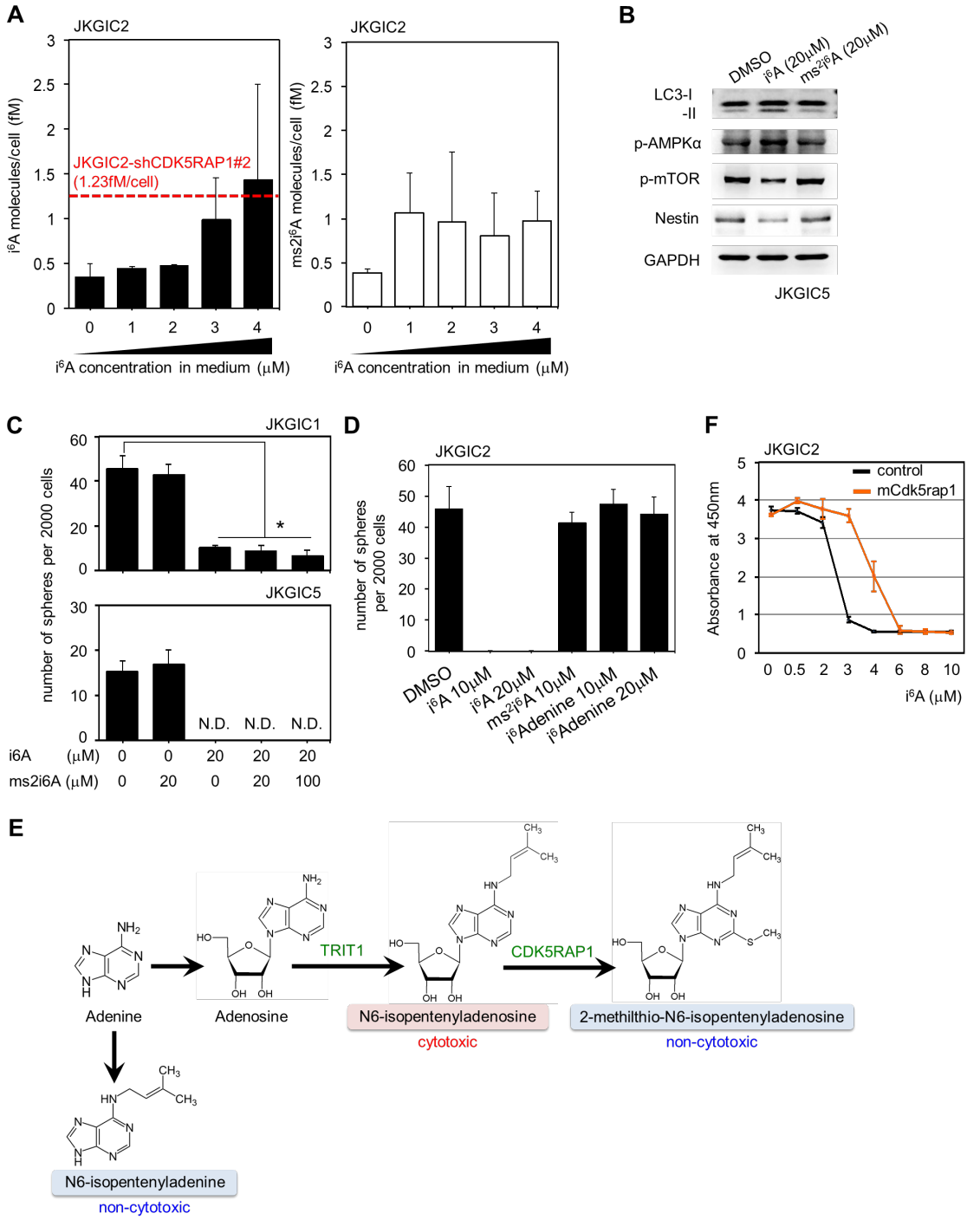
A
JKGIC2
i6A molecules/cell (fM)
JKGIC2-shCDK5RAP1#2
(1.23fM/cell)
i6A concentration in medium (μM)
JKGIC2
ms2i6A molecules/cell (fM)
i6A concentration in medium (μM)
B
DMSO
i6A (20μM)
ms2i6A (20μM)
LC3-I
-II
p-AMPKα
p-mTOR
Nestin
GAPDH
JKGIC5
C
JKGIC1
number of spheres per 2000 cells
JKGIC5
N.D.
i6A (μM)
ms2i6A (μM)
D
JKGIC2
number of spheres per 2000 cells
DMSO
i6A 10μM
i6A 20μM
ms2i6A 10μM
i6Adenine 10μM
i6Adenine 20μM
F
JKGIC2
control
mCdk5rap1
Absorbance at 450nm
i6A (μM)
E
Adenine
Adenosine
TRIT1
N6-isopentenyladenosine
cytotoxic
CDK5RAP1
2-methilthio-N6-isopentenyladenosine
non-cytotoxic
N6-isopentenyladenine
non-cytotoxic

Figure S4. Isopentenyl modification of the adenosine molecule alone results in cytotoxic effects, and i^6A is detoxified by 2-methylthio conversion via CDK5RAP1 (related to Figure 4).

(A) *Left*: i^6A treatment induced the intracellular concentration of i^6A in JKGIC2 cells in a dose-dependent manner. Note that the intracellular [i^6A] in JKGIC2 cells treated with 4 μM i^6A was consistent with that in shCDK5RAP1#2-JKGIC2 cells. *Right*: Intracellular concentration of ms^2i^6A in JKGIC2 cells treated with each concentration of i^6A. Exogenous i^6A did not affect the intracellular concentration of ms^2i^6A in a dose-dependent manner

(B) Treatment with i^6A, but not ms^2i^6A, activates the autophagic program and decreases the protein levels of Nestin in JKGIC5 cells.

(C) Quantification of primary spheres formed by JKGIC1 and JKGIC5 cells treated with i^6A or ms^2i^6A. Treatment with i^6A reduces the number of spheres, but this reduction is not rescued by the further addition of ms^2i^6A. Each bar represents the SD value from four independent replicates. *: $P<0.05$.

(D) Quantification of primary sphere formation by JKGIC2 cells (2,000/well) treated with i^6A, ms^2i^6A, and i^6Adenine. Treatment with i^6A but not ms^2i^6A or i^6Adenine reduces the number of spheres formed. Each bar represents the SD value from three independent replicates.

(E) Summary of the biochemical reactions related to the synthesis of i^6A, ms^2i^6A, and i^6Adenine.

(F) Effect of each concentration of i^6A on the growth of JKGIC2 cells overexpressing mouse Cdk5rap1 (mCdk5rap1). Overexpression of mCdk5rap1 protects cells from the inhibitory effect of 3 and 4 μM i^6A.

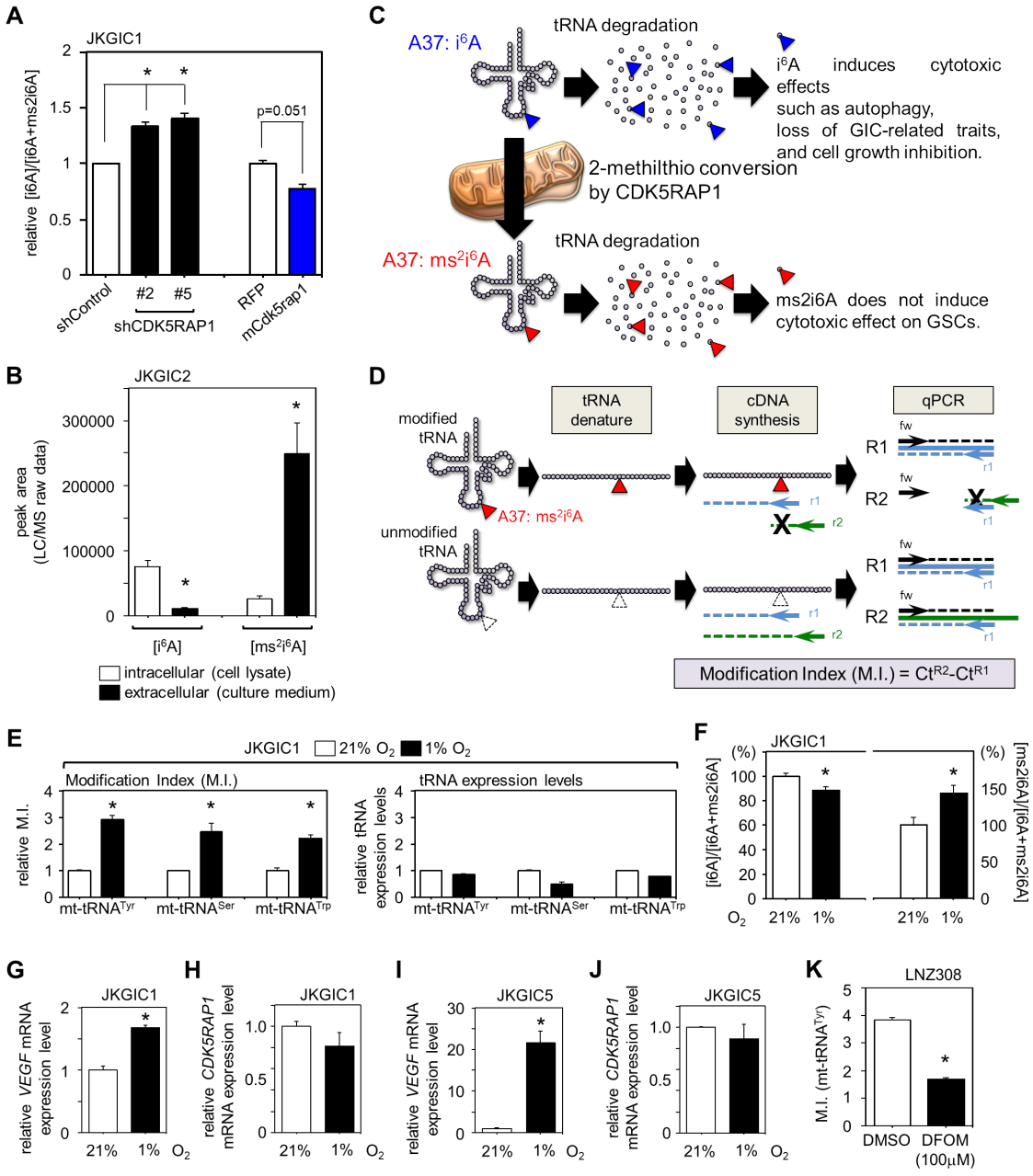
A
JKGIC1
relative [i6A]/[i6A+ms2i6A]
p=0.051
shControl
#2
#5
shCDK5RAP1
RFP
mCdk5rap1
B
JKGIC2
peak area (LC/MS raw data)
[i6A]
[ms2i6A]
intracellular (cell lysate)
extracellular (culture medium)
C
A37: i6A
tRNA degradation
i6A induces cytotoxic effects such as autophagy, loss of GIC-related traits, and cell growth inhibition.
2-methilthio conversion by CDK5RAP1
A37: ms2i6A
tRNA degradation
ms2i6A does not induce cytotoxic effect on GSCs.
D
tRNA denature
cDNA synthesis
qPCR
modified tRNA
A37: ms2i6A
unmodified tRNA
fw
R1
R2
r1
r2
Modification Index (M.I.) = CtR2-CtR1
E
JKGIC1 21% O2 1% O2
Modification Index (M.I.)
relative M.I.
tRNA expression levels
relative tRNA expression levels
mt-tRNATyr
mt-tRNASer
mt-tRNATrp
F
JKGIC1
[i6A]/[i6A+ms2i6A]
[ms2i6A]/[i6A+ms2i6A]
O2 21% 1%
G
JKGIC1
relative VEGF mRNA expression level
H
JKGIC1
relative CDK5RAP1 mRNA expression level
I
JKGIC5
relative VEGF mRNA expression level
J
JKGIC5
relative CDK5RAP1 mRNA expression level
K
LNZ308
M.I. (mt-tRNATyr)
DMSO
DFOM (100μM)

Figure S5. CDK5RAP1 controls the 2-methylthio modification of mt-tRNAs (related to Figure 5).

(A) Mass spectrometry analysis of [i^6A] and [ms^2i^6A] from the lysates of shControl- and shCDK5RAP1-, RFP-, mCdk5rap1-transfected JKGIC1 cells. Each bar represents the SD value from three independent replicates. *: $P<0.05$.

(B) LC/MS analyses of intracellular and extracellular concentrations of i^6A and ms^2i^6A. Note that ms^2i^6A is predominantly enriched in the cell culture medium. Each bar represents the SD value from three independent replicates.

(C) A model describing the molecular pathways that detoxify N6-isopentenyladenosine (i^6A). i^6A at position 37 in mt-tRNAs in the mitochondria is converted to ms^2i^6A by CDK5RAP1. Both i^6A and ms^2i^6A were produced by the degradation of mt-tRNAs.

(D) A schema describing the measurement of the M.I. of mt-tRNAs. For details, please see our previous report (Xie et al., 2013).

(E) The M.I. of ms^2i^6A corresponding each mt-tRNA, and tRNA expression level in JKGIC1 cells cultured in the presence of 21% and 1% O_2. The M.I.s in all CDK5RAP1-targeted tRNA species are increased under hypoxic conditions, but tRNA expression is not. The data are presented as the M.I. relative to the cells cultured under normoxia. Each bar represents the SD value from two independent replicates.

(F) Hypoxic conditions decrease intracellular [i^6A] and increase the secretion of ms^2i^6A by JKGIC1 cells. The data are presented as the percentage of the levels under normoxia. Each bar represents the SD value from three independent replicates. *: $P<0.05$.

(G-J) Hypoxic conditions significantly increased the expression levels of *VEGF* mRNA (G and I) but not *CDK5RAP1* mRNA (H and J) in JKGIC1 and JKGIC5 cells. Each bar represents the SD value from four independent replicates. *: $P<0.05$.

(K) Representative M.I. in LNZ308 cells treated with deferoxamine (100 μM). Each bar represents the mean of four replicates ± SD. *: $P<0.05$ *vs.* DMSO.

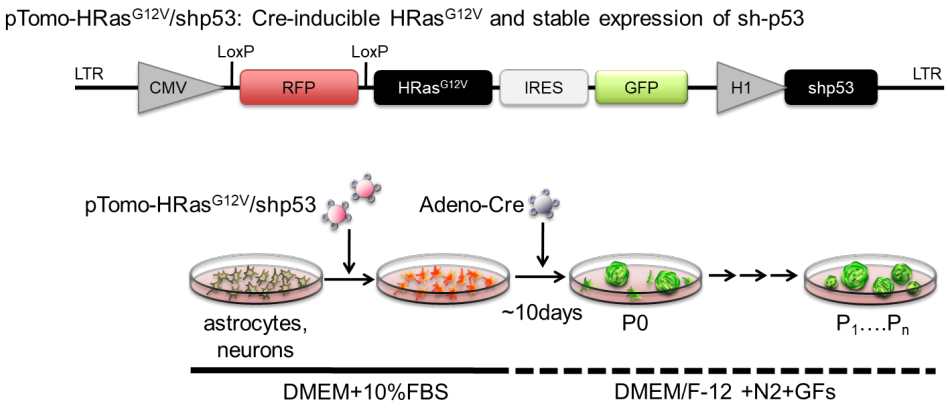

Figure S6. A schema representing the procedure of the gliosphere initiation assay (related to Figure 6).

TRANSPARENT METHODS

Cell Lines and Culture

Japan Kumamoto glioma-initiating cell (JKGIC) lines 1, 2, and 5 were used; these are patient-derived cell lines established at the Department of Neurosurgery, Kumamoto University Hospital. JKGIC1 cells were obtained from a 68-year-old male GBM patient, JKGIC2 cells were obtained from a 78-year-old female GBM patient, and JKGIC5 cells were obtained from a 70-year-old female GBM patient. The patients underwent tumor resection at our department, and primary GICs were cultured from the tumors. The tumors were washed with PBS (Thermo Fisher Scientific, Waltham, MA), cut into small pieces and minced. The minced tumors were subjected to trypsinization with 0.05% trypsin-EDTA (Wako, Tokyo, Japan) for 10 min at 37°C and plated. Study approval was obtained from the research ethics committee of Kumamoto University (Approval number: genome 231). GICs were grown in DMEM/Ham's F-12 with L-glutamine (Wako) supplemented with 10% BIT9500 (STEMCELL Technologies, Vancouver, Canada), 20 ng/ml basic fibroblast growth factor (Wako), 20 ng/ml epidermal growth factor (Wako), and 100 U/ml penicillin and streptomycin (Thermo Fisher Scientific) at 37°C in an environment containing 5% CO_2.

Xenograft experiments with patient-derived GICs.

For the xenograft tumor models, we used patient-derived GICs. We injected cells into 6-week-old female ICR-nu nu/nu mice and 6-week-old male BALB/c-nu

(CAnN.Cg-Foxn1^{nu}/CrlCrl)) mice to establish intracranial tumor xenograft models and subcutaneous xenograft models, respectively (all mice were obtained from Charles River Laboratories Japan, Yokohama, Japan). For the Kaplan-Meier analysis of survival, we defined endpoints as the time when the mice began to display neurological dysfunctions such as hemiparesis, were moribund or exhibited more than 20% weight loss. All procedures were approved by the Animal Ethics Committee of Kumamoto University (Approval ID: A29-016).

To generate the subcutaneous tumor xenograft model, we transduced JKGIC1, JKGIC2, and JKGIC5 cells with lentiviral vectors expressing shCDK5RAP1 or shControl. Equal numbers of cells (5 X 10^6 cells/100 μl) in PBS with 50% Matrigel® Matrix (Corning, Bedford, MA) were injected into both flanks (100 μl/side).

To generate the intracranial tumor xenograft model, we transduced JKGIC2 cells with lentiviral vectors expressing shCDK5RAP1 or shControl. The cells were diluted to equal concentrations (1 X 10^5 cells/μl) in PBS. At 1 to 2 weeks before cell injection, an implantable guide-screw system for intracranial injection was established as previously described (Lal et al., 2000). A 2.6-mm guide screw was implanted into a cranial hole made 2.5 mm lateral and 1 mm anterior to the bregma. Cells were injected (5 μl/hole of the guide screw) using a Hamilton syringe (Hamilton, Reno, Nevada).

Human Tissue Sample Collection and Studies

Tumor and peritumor (adjacent normal) tissues were collected from GBM patients treated at Kumamoto University Hospital. Tissues were used to assess gene expression levels, immunofluorescence staining, and mt-tRNA modifications as well as to perform LC-MS/MS. Approval was sought and obtained from the research ethics committee of Kumamoto University (Approval number: genome 231).

Mass spectrometry analysis of A, i^6A and ms^2i^6A.

Mass spectrometry analysis was performed to measure the levels of adenosine (A), N^6-isopentenyladenosine (i^6A) and 2-methylthio-N^6-isopentenyladenosine (ms^2i^6A) in the cell culture medium and tumor tissues. To extract nucleosides from the culture medium, we used a MonoSpin™ C18 (GL Sciences, Tokyo, Japan) according to the manufacturer's instructions. To extract intracellular nucleosides, we washed the cells three times with PBS and then homogenized them with 500 µl methanol. To extract nucleosides from tumor tissues, we homogenized the tissues by TissueRuptor (Qiagen, Venlo, Netherlands) in 500 µl methanol. The extracts were cleared by centrifugation at 10,000 rpm for 5 min. The supernatant was evaporated with a Savant Speed Vac SPD1010 (Thermo Fisher Scientific), and the pellet was resuspended in ultrapure water (Wako). The samples were analyzed with a triple-quadruple mass spectrometer (LCMS-8050, Shimazu, Kyoto, Japan) equipped with an electrospray ionization (ESI) source and a liquid chromatography system (Shimazu). A, i^6A and ms^2i^6A were detected by a multiple reaction monitoring (MRM) method in the positive ion mode.

The MRM parameters were as follows: A (precursor ion: m/z 268.0, product ion: m/z 136.0, collision energy: 17.0), i^6A (precursor ion: m/z 336.2, product ion: m/z 204.0, collision energy: 15.0), and ms^2i^6A (precursor ion: m/z 382.2, product ion: m/z 182.0, collision energy: 29.0).

i^6A and ms^2i^6A Treatment

GICs were seeded at approximately 80% confluence. The medium was removed and replaced with new medium containing different concentrations of i^6A (Wako) or ms^2i^6A (Wako). After 24 hours, immunocytochemical analysis was performed. Total proteins and nucleosides were extracted from cells 24 hours after i^6A and ms^2i^6A treatment. Sphere formation assays were performed one week after the treatment.

Lentiviral Preparation and Infection

Lentiviral vectors were used for gene silencing or gene expression. For lentivirus production, we cultured 293FT cells in DMEM (Thermo Fisher Scientific) supplemented with 10% FBS (Corning) and 100 U/ml penicillin and streptomycin (Thermo Fisher Scientific) at 37°C and 5% CO_2. Lentiviral vectors (10 μg) with the packaging vectors psPAX2 (7.5 μg) and pMD2.G (2.5 μg) were transiently transfected into 293FT cells using TransIT®-LT1 Transfection Reagent (Mirus Bio, Madison, WI) and Opti-MEM™ (Thermo Fisher Scientific). At 8-12 hours after transfection, the medium was changed. On the third day after transfection, viral supernatant was

collected and filtered through a 0.45 μm sterile filter unit containing a Durapore® PVDF membrane (Millipore, Darmstadt, Germany). Approximately 500-1,000 μl viral supernatant was used to infect GICs in a 25 cm^2 flask. The shRNA sequences are shown in the SUPPLEMENTAL TABLE (Table S1: Sequences).

Sphere Formation Assay

GICs were plated at 2,000 cells per well and grown at 37°C in an atmosphere containing 5% CO_2. After 1 week, the number of spheres per well (from 2,000 cells) was counted. To distinguish between independent spheres and improve our ability to count the number of spheres, we used ultra-low attachment 24-well plates (Corning). After the primary assay, the cells were replated at 2,000 cells per well, and secondary sphere formation assays were performed. For each condition, we prepared 4 technical replicates and performed 3 independent experiments unless otherwise noted.

Immunofluorescence Staining

Tissues were fixed overnight in formalin, embedded in paraffin and sliced into 4-μm-thick sections. After deparaffinization, Protease XXV (Thermo Fisher Scientific) was added to the sections for antigen retrieval, and the sections were then processed for immunofluorescence staining. The cells were fixed for 15 min at room temperature with 4% PFA, after which they were subjected to the following process: blocking with 5% donkey serum in PBST (0.2% Triton X-100 in PBS) for 1 hour at room temperature,

incubation with primary antibodies diluted with 5% donkey serum in PBST at 4°C overnight, and incubation with secondary antibodies diluted with 5% donkey serum in PBST at room temperature for 2 hours. The dilutions of primary and secondary antibodies were set according to the manufacturers' instructions. To label cell nuclei, we counterstained the samples with ProLong™ Gold Antifade Mountant with DAPI (Thermo Fisher Scientific). Images were obtained with an FV3000 confocal microscope (Olympus, Tokyo, Japan). A Fluorescein *In Situ* Cell Death Detection Kit (Sigma-Aldrich, St. Louis, Missouri) was used for the detection of apoptosis based on labeling of DNA strand breaks (TUNEL). The antibodies used are shown in the SUPPLEMENTAL TABLE (Table S2: Antibodies). For each experiment, we prepared 2 technical replicates and performed at least 2 independent experiments unless otherwise noted.

Immunoblotting (Western Blotting)

Proteins were extracted from cells with lysis buffer (20 mM Tris-HCL (pH 7.5), 1 mM EDTA-2Na, 1% Triton X-100, and PhosSTOP cocktail (1 tablet/10 ml)). The collected and lysed cells were homogenized with SONIFIER 250 (BRANSON, Danbury, CT) and cleared by centrifugation at 15,000 rpm and 4°C for 15 min. Protein concentrations were determined using a Pierce™ BCA Protein Assay Kit (Thermo Fisher Scientific). Equal amounts of proteins were electrophoresed on a 6-12% gradient acrylamide gel with Precision Plus Protein™ Dual Color Standards (Bio-Rad, Hercules, CA) and

transferred to PVDF membranes (Millipore). The membranes were blocked with 0.5% skim milk in TBST at room temperature for 1 hour, and blotting was performed by incubating the membranes with primary antibodies at 4°C overnight. Secondary antibodies were then incubated with the membranes at room temperature for 1 hour. Detection was performed with Amersham™ ECL™ Prime Western Blotting Detection Reagent (GE Healthcare, Fairfield, CT). The dilutions of the primary and secondary antibodies were used according to the manufacturers' instructions. The antibodies used are shown in the SUPPLEMENTAL TABLE (Table S2: Antibodies). We performed at least 2 independent experiments unless otherwise noted.

RNA Isolation and Quantitative RT-PCR

Total RNA from cells and tissues were isolated using TRIzol reagent (Thermo Fisher Scientific) and processed according to the manufacturer's instructions. The isolated RNA was diluted to 50 ng/μl. Recombinant DNase I (Takara, Shiga, Japan) was added to the isolated RNA and incubated for 20 min at 37°C. The RNA was then reverse-transcribed into cDNA using PrimeScript™ RT Master Mix (Takara). Quantitative RT-PCR was performed using gene-specific primers and SYBR Premix Ex Taq™ (Takara). The sequences of gene-specific primers (18S as a reference) are shown in the SUPPLEMENTAL TABLE (Table S1: Sequences). For each condition, we prepared 2 technical replicates and performed 2 independent experiments unless otherwise noted.

Modification Index of mitochondrial tRNA

To determine the ms^2i^6A modification in mitochondrial tRNAs, we adopted the quantitative PCR-based method, which we previously reported (Xie et al., 2013). Briefly, DNase I-treated total RNA were denatured at 65°C for 10min, and were used for cDNA synthesis with mitochondrial tRNA-specific primers (reverse r1 or reverse r2). Then, qPCR was performed with a primer set of forward (fw) and reverse r1 (rev1). The Ct number was obtained from the qPCR with cDNA templates of fw/rev1 and fw/rev2. The difference of the number of Ct(fw/rev1) and Ct(fw/rev2) is defined as the M.I. We reported that the M.I. reflected the absolute quantification of ms2 measured by mass-spectrometry.

Histology

Tumor and brain tissues were fixed overnight in formalin, embedded in paraffin and sliced into 4-μm-thick sections for histological examination. Hematoxylin and eosin (H&E) staining was performed with a standard method.

Assays to examine mitochondrial functions

The oxygen consumption rate (OCR) was determined with a Seahorse XF24 Analyzer (Agilent Technologies, Santa Clara, CA). JKGIC2 cells were plated at a density of 70,000 cells per well for measurement. Oligomycin (6.3 μM), FCCP (9 μM), rotenone

(5 μM) and antimycin (5 μM) were used as metabolic inhibitors. All assays were performed according to the manufacturer's instructions.

Electron microscopy

JKGIC2 cells were transduced with lentiviral vectors expressing shCDK5RAP1 or shControl. At 4 days after infection, the cells were fixed with 2% glutaraldehyde and 2% paraformaldehyde, further fixed with osmium tetroxide, embedded in epoxy resin, sliced, and examined with an electron microscope (HITACHI Electron Microscope Model H-7650).

Quantification and statistical analyses.

The data were analyzed using Microsoft Excel (Microsoft, Washington), GraphPad Prism (GraphPad, La Jolla, CA) and StatMate III (ATMS, Tokyo, Japan) software. Data are expressed as the mean ± SD. Student's *t* test was used to assess the differences between two groups. One-way analysis of variance (ANOVA) was used to assess the differences among multiple groups followed by t-test with Bonferroni correction of the *P* value between two groups. The log-rank test and Kaplan-Meier method were used to compare the survival distributions between two groups. $P < 0.05$ was considered statistically significant.

SUPPLEMENTAL REFERENCES

Xie, P., Wei, F.Y., Hirata, S., Kaitsuka, T., Suzuki, T., Suzuki, T., Tomizawa, K. (2013). Quantitative PCR measurement of tRNA 2-methylthio modification for assessing type 2 diabetes risk. Clin Chem 59, 1604-1612.

Murata, H., Yoshimoto, K., Hatae, R., Akagi, Y., Mizoguchi, M., Hata, N., Kuga, D., Nakamizo, A., Amano, T., Sayama, T., Iihara, K. (2015). Detection of proneural/mesenchymal marker expression in glioblastoma: temporospatial dynamics and association with chromatin-modifying gene expression. J. Neurooncol 125:33-41.

Table S1. Sequences of Primer and shRNA. Related to methods.

The ribosomal 18S gene was used as a reference gene for quantitative RT-PCR.

Primers	Sequences
Cdk5rap1 (Human) forward	ATGGCTGCCAGATGAATGTGA
Cdk5rap1 (Human) reverse	CTCTTGGAGGTTACTGGTCCG
Cdk5rap1 (Mouse) forward	CCATGTGCTGGGTGTTGCTTA
Cdk5rap1 (Mouse) reverse	TCTGCCTTCCTAGAAGTTCATCC
18S forward	GTAACCCGTTGAACCCCATT
18S reverse	CCATCCAATCGGTAGTAGCG
Sox2 forward	TACAGCATGTCCTACTCGCAG
Sox2 reverse	GAGGAAGAGGTAACCACAGGG
Olig2 forward	TGGCTTCAAGTCATCCTCGTC
Olig2 reverse	ATGGCGATGTTGAGGTCGTG
POU3F2 forward	CGGCGGATCAAACTGGGATTT
POU3F2 reverse	TTGCGCTGCGATCTTGTCTAT
SALL2 forward	CCCCTGATCTTGGAAGAGCTA
SALL2 reverse	CACCGTCTGGCCTAAGGAG
CD44 forward	TCCAACACCTCCCAGTATGACA
CD44 reverse	GGCAGGTCTGTGACTGATGTACA
CD133 forward	TTCTTGACCGACTGAGACCCA
CD133 reverse	TCATGTTCTCCAACGCCTCTT
VEGF forward	AGGGCAGAATCATCACGAAGT
VEGF reverse	AGGGTCTCGATTGGATGGCA
DLL3 forward	ACATGTGCAGATGGACCCTG
DLL3 reverse	AAAAGGTAGCGCTGAGGGTC
BCAN forward	ACCTAGCATCCCCATCACCT
BCAN reverse	GAAGTCCTGTTCCTCGGGTG
NCAM1 forward	CCTATCCCAGTGCCACGATC
NCAM1 reverse	ATCCTCTCCCATCTGCCCTT
NKX2.2 forward	ACCAACACAAAGACGGGGTT
NKX2.2 reverse	TGTAGCGGTGGTTCTGGAAC
ASCL1 forward	CAGCCTGTTTCTTTGCCACG

ASCL1 reverse	GTCGTTGGAGTAGTTGGGGG
CHI3L1 forward	TACGGCATGCTCAACACACT
CHI3L1 reverse	TGCCCATCACCAGCTTACTG
VIM forward	CTCTGGCACGTCTTGACCTT
VIM reverse	ACGAAGGTGACGAGCCATTT
RelB forward	CATCAGAGCTGCGGATTTGC
RelB reverse	GACACGGTGCCAGAGAAGAA
TRADD forward	CAGCAGAAGGTGGCAGTGTA
TRADD reverse	CACCTTGCGCCATTTGAGAC
PDPN forward	AGGTGCCGAAGATGATGTGG
PDPN reverse	GCGAGTACCTTCCCGACATT
mt-tRNATyr forward	GCTGAGTGAAGCATTGGACT
mt-tRNATyr reverse r1	AACCCCTGTCTTTAGATTTACA
mt-tRNATyr reverse r2	AGAGGCCTAACCCCTGTCTT
mt-tRNASer forward	GAGGCCATGGGGTTGG
mt-tRNASer reverse r1	CCCAAAGCTGGTTTCAAGC
mt-tRNASer reverse r2	AATCGAACCCCCCAAAGC
mt-tRNATrp forward	GGTTAAATACAGACCAAGAGC
mt-tRNATrp reverse r1	CAACTTACTGAGGGCTTTGAA
mt-tRNATrp reverse r2	TTAAGTATTGCAACTTACTGAGG
shRNA	**Sequences**
shCDK5RAP1 #1 (Human)	CCGGGGCTTTACCACCAACTATAAACTCGAGTTTATAGTTGG TGGTAAAGCCTTTTT
shCDK5RAP1 #2 (Human)	CCGGCCAATCTCAGTCGTGGCTTTACTCGAGTAAAGCCACGA CTGAGATTGGTTTTT
shCDK5RAP1 #5 (Human)	CCGGTGGAGTTAGTTCACCATATTACTCGAGTAATATGGTGA ACTAACTCCATTTTT

shTUFM #1 (Human)	CCGGGCTCACCGAGTTTGGCTATAACTCGAGTTATAGCCAAACTCGGTGAGCTTTTT
shTUFM #2 (Human)	CCGGCAGCCAATGATCTTAGAGAAACTCGAGTTTCTCTAAGATCATTGGCTGTTTTT
shTSFM #1 (Human)	CCGGCTCCTTTGTAAATTGCAAGAACTCGAGTTCTTGCAATTTACAAAGGAGTTTTT
shTSFM #2 (Human)	CCGGCAGGAAGGAAACACAACTGTACTCGAGTACAGTTGTGTTTCCTTCCTGTTTTT
shAtg5 #1 (Human)	CCGGCCTGAACAGAATCATCCTTAACTCGAGTTAAGGATGATTCTGTTCAGGTTTTT
shAtg5 #2 (Human)	CCGGCCTTTCATTCAGAAGCTGTTTCTCGAGAAACAGCTTCTGAATGAAAGGTTTTT

Table S2. The antibodies used. Related to methods.

Antibodies	SOURCE	IDENTIFIER	Dilutions
Anti-GAPDH	Santa Cruz Biotechnology	Catalog # sc-47724	WB (1:1000)
Anti-Nestin	Sigma-Aldrich	Catalog # N5413	WB (1:1000) IF (1:200)
Anti-Sox2	Santa Cruz Biotechnology	Catalog # sc-17320	WB (1:1000) IF (1:100)
Anti-Olig2	R&D Systems	Catalog # AF2418	WB (1:1000)
Anti-Brn2/POU3F2	Cell Signaling Technology	Catalog # 12137S	WB (1:1000)
Anti-SALL2	Bethyl	Catalog # A303-208A	WB (1:1000)
Anti-YAP/TAZ	Cell Signaling Technology	Catalog # 8418	IF (1:100)
Anti-MTCO1	Abcam	Catalog # ab14705	WB (1:1000)
Anti-Cleaved Caspase-3	Cell Signaling Technology	Catalog # 9661	WB (1:1000)
Anti-mTOR	Cell Signaling Technology	Catalog # 2983	WB (1:1000)
Anti-mTOR, phospho	Cell Signaling Technology	Catalog # 2976	WB (1:1000)
Anti-p70 S6 Kinase	Cell Signaling Technology	Catalog # 2708	WB (1:1000)
Anti-p70 S6 Kinase, phospho	Cell Signaling Technology	Catalog # 9208S	WB (1:1000)
Anti-Human LC3	MBL International	Catalog # PM036	WB (1:1000) IF (1:200)
Anti-AMPK alpha	Cell Signaling Technology	Catalog # 2535	WB (1:1000)
Anti-AMPK-alpha, phospho	Cell Signaling Technology	Catalog # 5831	WB (1:1000)
Anti-ms^2i^6A	Millipore	Catalog # MABS1280	IF (1:100)
Anti-Cytochrome b	Santa Cruz	Catalog # sc-9509	WB (1:1000)

Anti-ND6	Santa Cruz	Catalog # sc20510-R	WB (1:1000)
Anti-Mouse IgG	Dako	Catalog # P0447	WB (1:2000)
Anti-Rabbit IgG	Thermo Fisher Scientific	Catalog # P2771MP	WB (1:2000)
Anti-Goat IgG	Dako	Catalog # P0449	WB (1:2000)
Anti-Goat IgG, Alexa Fluor 555	Thermo Fisher Scientific	Catalog # A-21432	IF (1:500)
Anti-Rabbit IgG, Alexa Fluor 488	Thermo Fisher Scientific	Catalog # A-11034	IF (1:500)
Anti-Rabbit IgG, Alexa Fluor 555	Thermo Fisher Scientific	Catalog # A-21429	IF (1:500)
Anti-Mouse IgG, Alexa Fluor 488	Thermo Fisher Scientific	Catalog # A-11029	IF (1:500)